AD-A078 294 PHOENIX CORP MCLEAN VA F/G 8/3
VALIDATION OF OCEAN TIDE MODELS FROM SATELLITE ALTIMETRY.(U)
OCT 79 R D BROWN N00014-79-C-0409
UNCLASSIFIED NL

| OF |
AD-
A078294

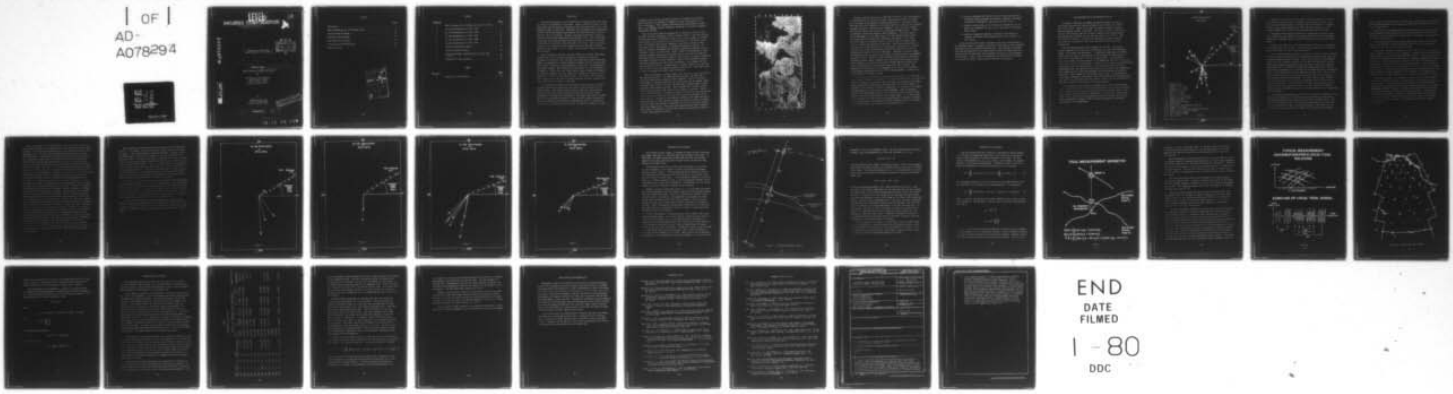

END
DATE
FILMED
1-80
DDC

LEVEL II

PHOENIX CORPORATION
1600 ANDERSON ROAD, McLEAN, VIRGINIA 22102
(703) 790-1450 • TWX 710-833-0323

(12)

(6) Validation of Ocean Tide Models From Satellite Altimetry.

(10) R. D. Brown

(9) Interim Progress Report. May - Oct 78,

Under Contract No. N00014-79-C-0409

(15)

to

The Office of Naval Research
Earth Physics Program
800 N. Quincy Street
Arlington, Virginia 22217

by

Phoenix Corporation
1700 Old Meadow Road
McLean, Virginia 22102

(11) 15 October 15, 1979 (12) 36

409 911 mt

CONTENTS

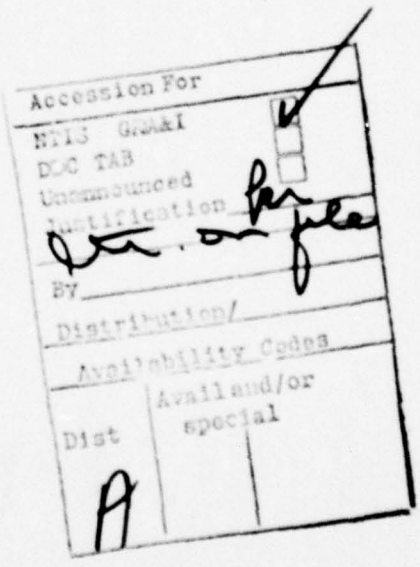

FIGURES

TABLE

INTRODUCTION

The principal obstacle to the construction of accurate global tide models is the lack of observations in mid-ocean. There is currently a wealth of tide gauge data from the shores and estuaries of most developed countries and a few scattered islands in mid-ocean. These data have occasionally been supplemented by data from bottom pressure gauges emplaced for relatively short periods of time at a very few locations. Recently, land-based tidal gravity data have also been used in tidal modeling (Kuo and Jachens [1977]). But to model deep ocean tides from these essentially land-based data is analogous to modeling a hurricane in mid-ocean by observing swell at the shore. Only the grossest features can be depicted and many assumptions must be made which limit the accuracy of such models. This is evident from a review of present tide modeling techniques.

Many investigators (Pekeris and Accad [1969], Zahel [1970], Hendershott [1966], Estes [1977]) have developed global tide models by numerical integration of LaPlace's tidal equations, but these models require additional models (or assumptions) of related physical parameters such as coastline geometry, bottom topography, energy dissipation, earth tides, self-gravitation, and crustal loading. Their sensitivity to uncertainty in these parameters can be dramatic. Pekeris and Accad [1969] find that small changes in dissipation or coastline parameters can cause amplitudes to change by a factor of 3 and amphidromes to rotate in the wrong direction. As a result, Kuo and Jachens [1977] among others, find that such models generally give poor agreement with tidal observations on islands in mid-ocean.

In an alternative approach, Kuo and Jachens [1977] recently used tidal gravity observations to model open ocean tides in limited regions of the world's oceans. This approach models only the relatively long wavelength features of the ocean tides (typically 1800 km or more in scale length) depending on the number and distribution of land based tidal gravity stations. Since it is an inversion technique, it does not yield unique solutions and must be constrained by bottom pressure observations, and it is sensitive to the location of the tidal gravity stations. An important assumption of this

technique is that the tide outside the region to be modeled is accurately known, and thus this technique is dependent on other tidal models for the rest of the globe. Other regional tide models using bottom pressure gauges (Munk, et al [1970]), require unrealistic smoothing of the bottom topography (Hendershott, [1973]).

Many of the above mentioned problems may be solved by the use of direct satellite altimetry measurements (Zetler and Maul [1971]). Since the satellite altitude measurement is referenced to the earth's center of mass, such measurements yield the true elevation of sea surface relative to this point, and are free of assumptions about bottom topography, earth tides, crustal loading, coastlines, and the distribution of terrestrial measurement stations. In addition, satellite measurements can be made at high spatial density over all the world's oceans in a short time. Figure 1 shows the distribution of GEOS-3 satellite altimeter measurements resulting from the first year of operation. This satellite was just recently turned off after more than 4 years of operation. The Seasat satellite, which was launched in June of 1978, produced altimeter data which supplements the GEOS-3 data distribution. Even though this satellite operated only 99 days, altimeter data to a spatial density of 50 km, from 72°N to 72°S latitude was produced uniformly over the globe. This data serves to fill in the gaps in the GEOS-3 data distribution.

While the altimetric technique showed great potential, it also had formidable practical problems. The simulation study by Zetler and Maul [1971], showed that amplitudes and phases of tidal components could be recovered in the presence of realistic satellite orbit errors, but Maul and Yanaway [1978] found that actual orbit errors were too large and not random enough to permit successful tide parameter recovery. They concluded that 1 m orbit accuracy must be achieved before tidal recovery from altimetry is possible. Won and Miller [1978] attempted to mitigate the effects of orbit error by simultaneously solving for geoid, tides, and bias type orbit errors from altimetry in the North Atlantic. Although they achieved good agreement with independent geoid models and reduced tidal amplitude residuals to less than a meter, the agreement with known tide parameters, especially the M_2 tide in the North Atlantic area, was disappointing. They cited insufficient altimeter data, excessive orbit errors, and excessive altimeter data noise as the principal reasons for the poor tidal parameter recovery.

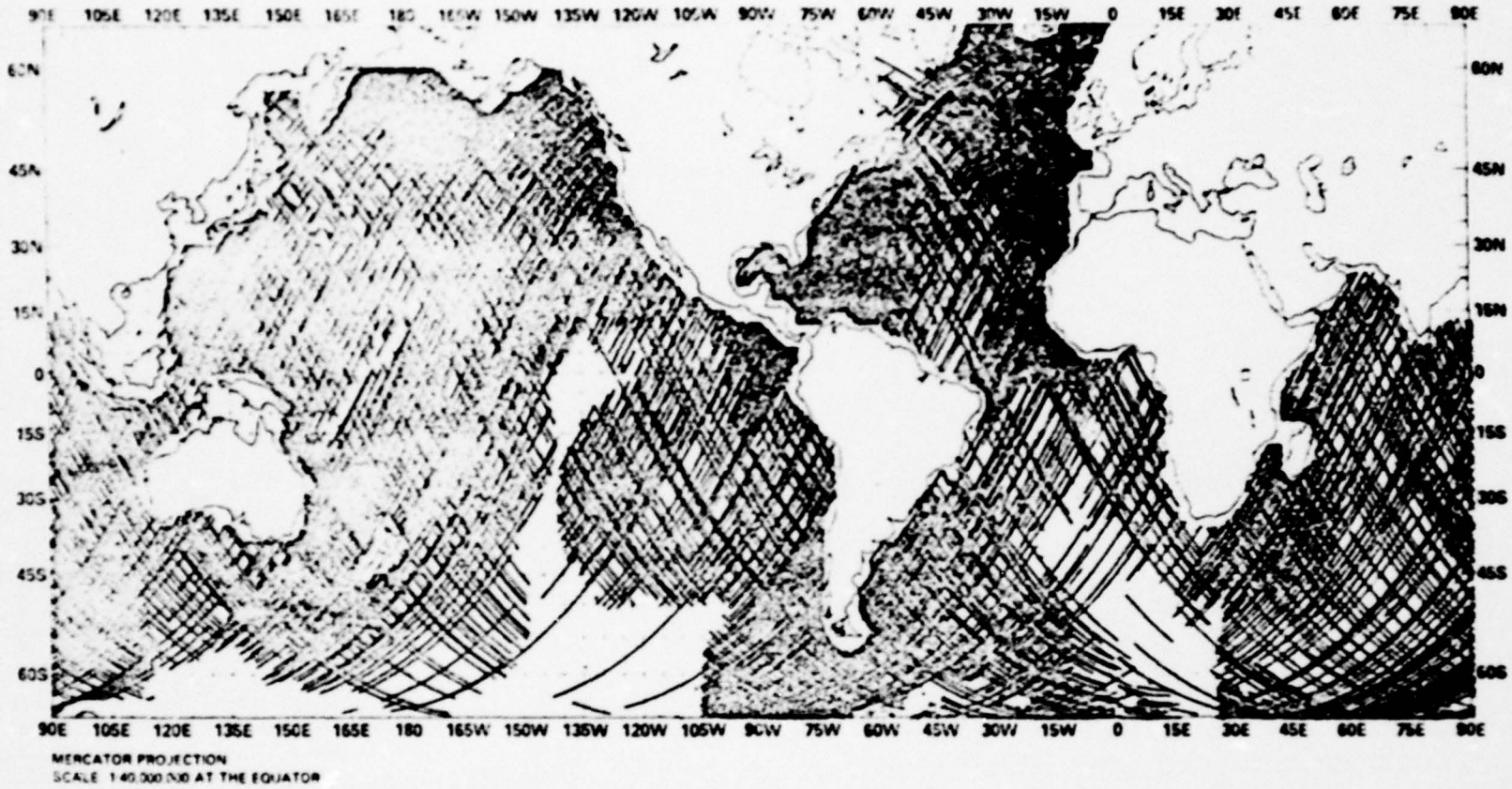

Figure 1. GEOS-3 Altimeter Data Distribution from 4/75 to 6/76

Recently, however, Brown and Lo [1978] were successful in the determination of tidal parameters in the Gulf of Alaska, from analysis of GEOS-3 altimeter data, by using a unique method for removing orbit errors. Each pass of altimeter data was first converted to sea surface heights, by using an initial (albeit erroneous) estimate of satellite orbit ephemeris. These sea surface height data are then fitted, pass by pass, to a model geoid height surface. The fit is effected by varying the satellite orbit parameters. Since each pass is fitted independently to the same surface, all long wavelength orbit errors are removed while preserving short wavelength tide signals. After orbit errors are removed, an approach similar to that of Maul and Yanaway [1978] is used to define tidal phases and amplitudes. Tidal phases are defined by analysis of sea height differences at intersections (crossovers) of satellite subtracks, and a least squares harmonic analysis is conducted to solve for amplitudes and phases of the tidal components. Estimates of the tidal phase and amplitude from 6 locations in this region were generated from a preliminary collection of data. Results at these locations, representative of different bathymetric regimes, agree in general with the bottom pressure gauge measurements of Rapatz, et al [1977] in the Gulf of Alaska seamount province, and confirm the existence of 4 meter tidal range in the Gulf of Alaska. In a separate test, recovery of M_2 tide parameters at the location of the MODE 3 bottom pressure gauge (Zetler, et al [1975]) showed agreement to within 26 cm in amplitude and 30 degrees in phase.

This approach is extended in this study to 26 locations in the Northeast Pacific Ocean. While it is sensitive to the altimeter data accuracy and the distribution of crossovers in space and time, it is much less sensitive to satellite orbit errors than the techniques of Won and Miller, or Maul and Yanaway. In addition, in its reliance on crossover comparisons, it is immune to the effects of sharp gradients in the geoid or bottom topography. Since it generates strictly local quasi-point solutions, it can be done quickly and efficiently, without the need for modeling effects in a larger region. It can also create global tide maps to a very fine scale by doing separate local point solutions at the required spatial separation, and is not inherently limited to regional or local application. The objectives of this study are to:

- develop a technique for low-cost survey of ocean tide phenomena of long and short wavelength in mid-ocean, completely independent from models of bathymetry, coast lines, and earth lines
- produce a detailed map of the co-tidal and co-range lines of the major tidal components (M_2, K_1, S_2, O_1, and N_2) in the Northeast Pacific Ocean
- provide a comparative analysis of altimetric tide models and existing tide models in the Northeast Pacific for validation of these models.

In the sections which follow, the state of the art in tide modeling in the Northeast Pacific is reviewed, followed by a discussion of data processing performed to date on the GEOS-3 altimeter data. The locations of potential tide solutions permitted by the distribution of GEOS-3 and SEASAT satellite altimeter data are identified, and preliminary solutions of tide parameters are discussed. Finally, plans for completing the validation of tide models in the Northeast Pacific using satellite altimetry are presented.

TIDE DETERMINATION IN THE NORTHEAST PACIFIC

To provide a reference for judging altimetric solutions for tides, we review here the results of previous attempts to model tides in the Northeast Pacific Ocean. Rather than compare the models everywhere, a single common geographic location is selected. This point is chosen in deep ocean, at about 215°W longitude and 34°N latitude, because bottom pressure guage measurements were available for this location (Irish, et al [1971]). This is the JOSIE II station. A single point comparison also better serves to illustrate the uncertainty in deep ocean tide models, rather than their similarities.

Most investigators model the M_2 component of the tide. This is the largest component of the tides, but unfortunately, the least well determined Figure 2 illustrates this uncertainty. M_2 amplitudes (indicated by the arrow length) and phase angles (indicated by the arrow direction) range from 13 to 57 cm and are scattered over a 300° arc of phase angles. This situation is due to two factors, the near resonance of the semidiurnal tide (M_2, S_2, N_2, etc.) in this part of the ocean (Hendershott, [1973]), and the indirect tide determination techniques used by most investigators. Since most investigators use tide measurements which are rather far removed from the deep ocean, many assumptions and auxiliary physical models are necessary in the calculation of the tide in deep water. Small changes in these models, such as coast line configuration, ocean depth, dissipation, earth tides, ocean bottom loading, and self-attraction, can lead to tidal amplitudes that fluctuate by 3 meters or more, and amphidromes that shift location or even rotate in the wrong direction.

It is instructive to review the techniques used in these tide determinations. Proceeding in more or less chronological order, the earliest techniques are the semi-empirical techniques of Harris [1904] and Dietrich [1944]. Only phase angles (co-tidal lines), not amplitudes, were determined. Observed tide phases at the coasts and at some islands were used to determine the co-tidal lines of amphidromic systems. These lines were extrapolated to determine the locations of the amphidrome.

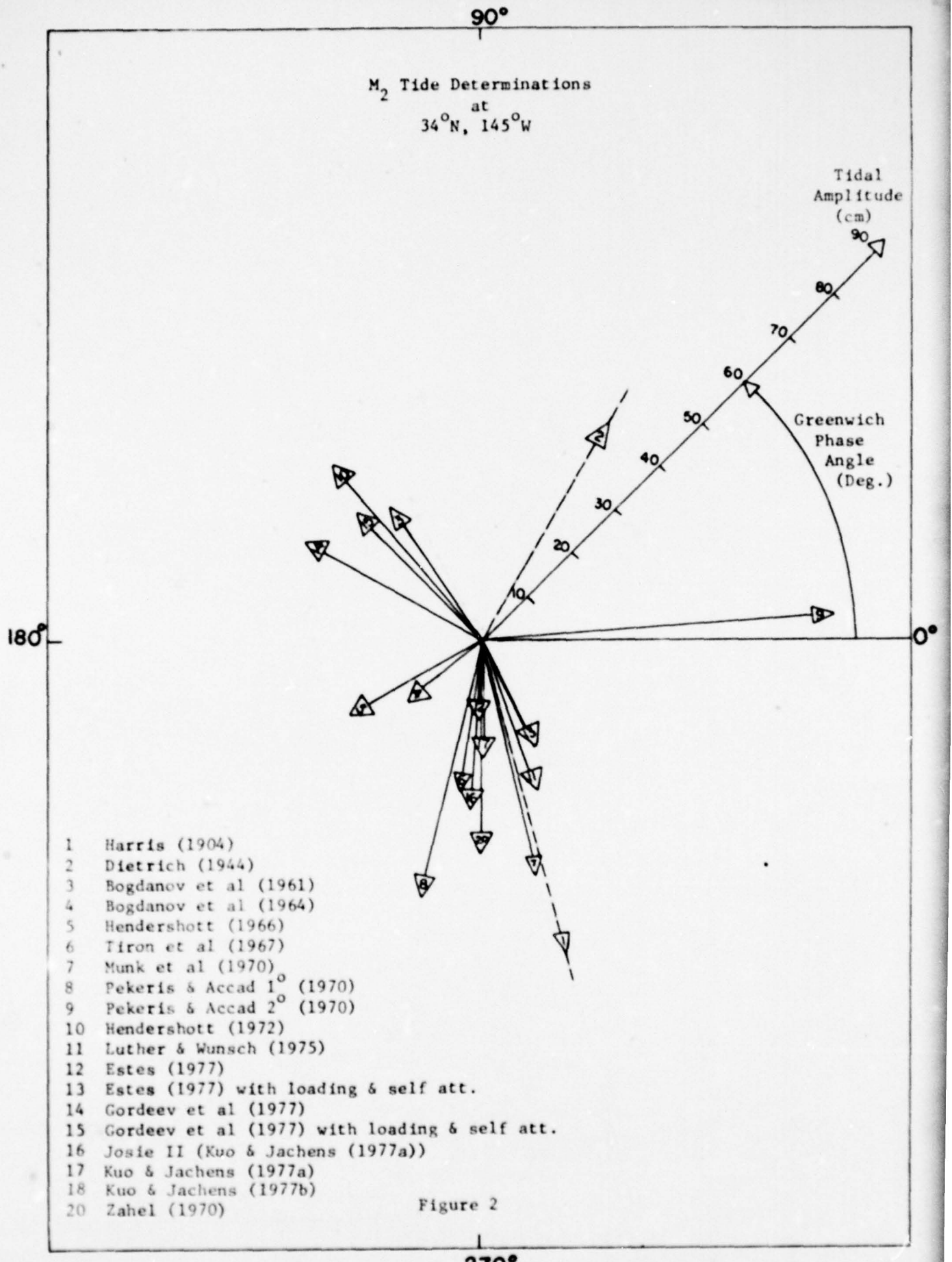

1 Harris (1904)
2 Dietrich (1944)
3 Bogdanov et al (1961)
4 Bogdanov et al (1964)
5 Hendershott (1966)
6 Tiron et al (1967)
7 Munk et al (1970)
8 Pekeris & Accad 1° (1970)
9 Pekeris & Accad 2° (1970)
10 Hendershott (1972)
11 Luther & Wunsch (1975)
12 Estes (1977)
13 Estes (1977) with loading & self att.
14 Gordeev et al (1977)
15 Gordeev et al (1977) with loading & self att.
16 Josie II (Kuo & Jachens (1977a))
17 Kuo & Jachens (1977a)
18 Kuo & Jachens (1977b)
20 Zahel (1970)

Figure 2

Bogdanov et al [1961a,b], [1964] used the harmonic constants of the tide at coastal and island stations to determine the instantaneous relief of the ocean surface (isohypse method). Co-tidal lines were determined by comparing isohypse charts at appropriate times. Where data were lacking, as on the southern boundary of the world's oceans, interpolated values were used.

Hendershott [1966] used the principles of hydrodynamics (numerical solution of Laplace's tidal equation) in a global solution for tides in idealized ocean basins. Observed tides at coastal stations were used as boundary conditions.

Tiron et al [1967] also used a global numerical solution a la Hendershott, but included island data as well. Dissipation was parameterized by specifying coastal elevations, and earth tides were ignored.

The tide determinations by Munk et al [1970] were local in nature, confined to the area along the California coast between San Francisco and San Diego, and extending westward halfway to Hawaii. Rather than relying on coastal measurements, which they regarded as anomalistic for deep ocean modeling, they used bottom pressure gauge measurements at eight stations in deep water beyond the continental shelf. The model is a normal mode representation of the coastal tide, without dissipation, but accounting for the earth tide due to astronomical forces. Their model predicted an M_2 amphidrome at about 27°N, 135°W. To test this prediction, Irish et al [1971] placed several deep sea bottom pressure gauges around the predicted amphidrome. The record from one gauge (JOSIE II at 34°N, 145°W) seaward of the predicted amphidrome showed that indeed there was a phase difference of 160° between this location and measurements on the opposite side of the amphidrome. However, the tide constants for JOSIE II differ from that predicted by Munk et al for this location by 14 cm in amplitude and 18° in phase.

The solution by Pekeris and Accad [1970] is a numerical integration of the Laplace tidal equations for the globe, with no earth tides, but with tidal dissipation parameterized as linearized bottom stress in shallow water. They used a fairly detailed model of the ocean bottom topography, but did not use coastal observations of tides as boundary conditions. They found that the predicted tide is very sensitive to changes in the coastline configuration.

This is evident in Figure 2, from the difference in amplitude (14 cm) and phase (107^{o}) between solutions 8 and 9, where the coast lines are modeled on a 1^{o} and 2^{o} grid respectively.

Hendershott [1972] modified Laplace's tidal equations to account for ocean bottom loading and self-attraction as well as the astronomical forces in the yielding of the ocean bottom due to earth tides. Dissipation was parameterized as a near coastal process.

Luther and Wunsch (1975) constructed updated tidal charts for the Pacific using a semi-empirical technique similar in concept to those of Harris and Dietrich but with more recent tidal observations.

Estes [1977] extended the approach of Zahel [1970] to the O_1, P_1, K_2, S_2, and N_2 components as well as the M_2 component. Self-attraction and ocean bottom loading were also included following Hendershott [1972]. These effects on the ocean tide determination can be quantified by comparing determinations 12 and 13 in Figure 2. A shift in amplitude and phase of 6 cm and 27^{o} respectively is observed due to self-attraction and ocean bottom loading. This is similar in magnitude to the change in the determinations 14 and 15 by Gordeev et al [1977] (3 cm and 16^{o}). These latter investigators also used self-attraction and ocean bottom loading following Hendershott, but the treatment of dissipation was similar to that of Pekeris and Accad, i.e., bottom stress linear with velocity.

The final technique to be considered is that of Kuo and Jachens [1977a] who used the variation of gravity on land to deduce the amplitude and phase of the ocean tide. It has long been known that ocean bottom loading affects surface gravity measurements, even at intercontinental distances. By a linear programming inversion technique, components of the tides can be mapped from tidal gravity signals at a network of terrestrial stations. The results of this technique are somewhat sensitive to the distribution of these stations and to the tide model assumed for oceans outside the region to be modeled, but it does yield good agreement with independent bottom pressure gauge measurements.

With the exception of the determination number 16, which is from a bottom pressure gauge located at the comparison point, all other determinations shown in Figure 2 were made from observations which are considerably distant from the comparison point. The wide spread in amplitudes and phases for this point are due primarily to differences in techniques used in these determinations. It is interesting to note that the earliest and the latest determinations (Harris, [1904], and Kuo and Jachens [1977] are only 14 degrees different in phase. One might conclude that tide determinations themselves have a periodicity of 70 years! There seems to be a slight preference among the determinations for the 270^{o} phase angle, in agreement with the JOSIE II data but it is hard to rule out determinations 2 through 5, 9 & 10, and 14 & 15 as being invalid. It has been speculated (Munk, et al [1970]) that the use of coastal tide observations for deep ocean tide determination is questionable because of the severe local anomalies that can occur in coastal environments. It is a fact that most coastal tide gauges are located in estuaries or bays that are protected from the waves and winds of the open ocean. They are also protected from the open ocean tide by up to 60 degrees of phase difference. A similar situation exists for tide gauges on islands. They are usually placed inside lagoons or in narrow straits between islands for local navigation purposes. These observations can have 30 to 60 degrees phase difference from the tide in the adjacent open ocean (Gallagher et al [1971]). But those tide determinations reviewed above which depend on these observations as boundary conditions show no distinctive distribution of amplitude or phase which might distinguish them as a class from the other types of solutions. Neither do the empirical solutions appear better or worse than the numerical solutions. There appears to be no preferred technique among the tide determinations examined here. Their variance appears to arise from the near resonance of the M_2 tide in the Northeast Pacific responding to small differences in treatment of dissipation, and is probably most sensitive to the parameterization of coast lines. Hendershott, [1973] recommends that small details such as accurate models of the continental shelf and island scattering and diffraction be developed before proceeding to develop deep water tide models using the techniques described above.

The situation is much the same for the S_2 semi-diurnal tide components (Figure 3). The numbers in this and subsequent figures refer to the legend in Figure 2. Again a wide spread in amplitude and phase is evident, with no preferred values. Perhaps the S_2 component is also near resonance in the Northeast Pacific. The other tide components examined seem to show preferred values for amplitude and phase, although this is inconclusive because of the smaller number of determinations. The N_2 component (Figure 4), is determined by only 2 investigators, and they report values of 4 cm $\pm$ 1 cm and $268^{\circ} \pm 1^{\circ}$ for N_2 amplitude and phase. The diurnal tide components, K, and O_1 (Figures 5 and 6 respectively) show a marked preference for 240° in phase and 29 cm and 16 cm, respectively, for amplitude. Presumably, the Northeast Pacific Ocean basin is not resonant for these components of the tide.

It should be noted that most of these tide parameters have been extracted from published tide charts of co-tidal and co-range lines. These charts have varying resolution capability, and interpolated values of amplitude and phase are of varying accuracy. A conservative estimate of the accuracy of these parameters would be $\pm$ 5 cm for amplitude and $\pm 5^{\circ}$ for phase angle. In other words, the accuracy of reading these charts usually exceeds the accuracy of the charts themselves, especially in the case of the M_2 tide.

Given this state-of-the-art in tide determinations in the Northeast Pacific, altimeter tide determinations can only improve our knowledge of the M_2 and S_2 components. The best tests for evaluating the altimeter technique appear to be comparison with K_1, O_1 and perhaps N_2 determinations discussed above.

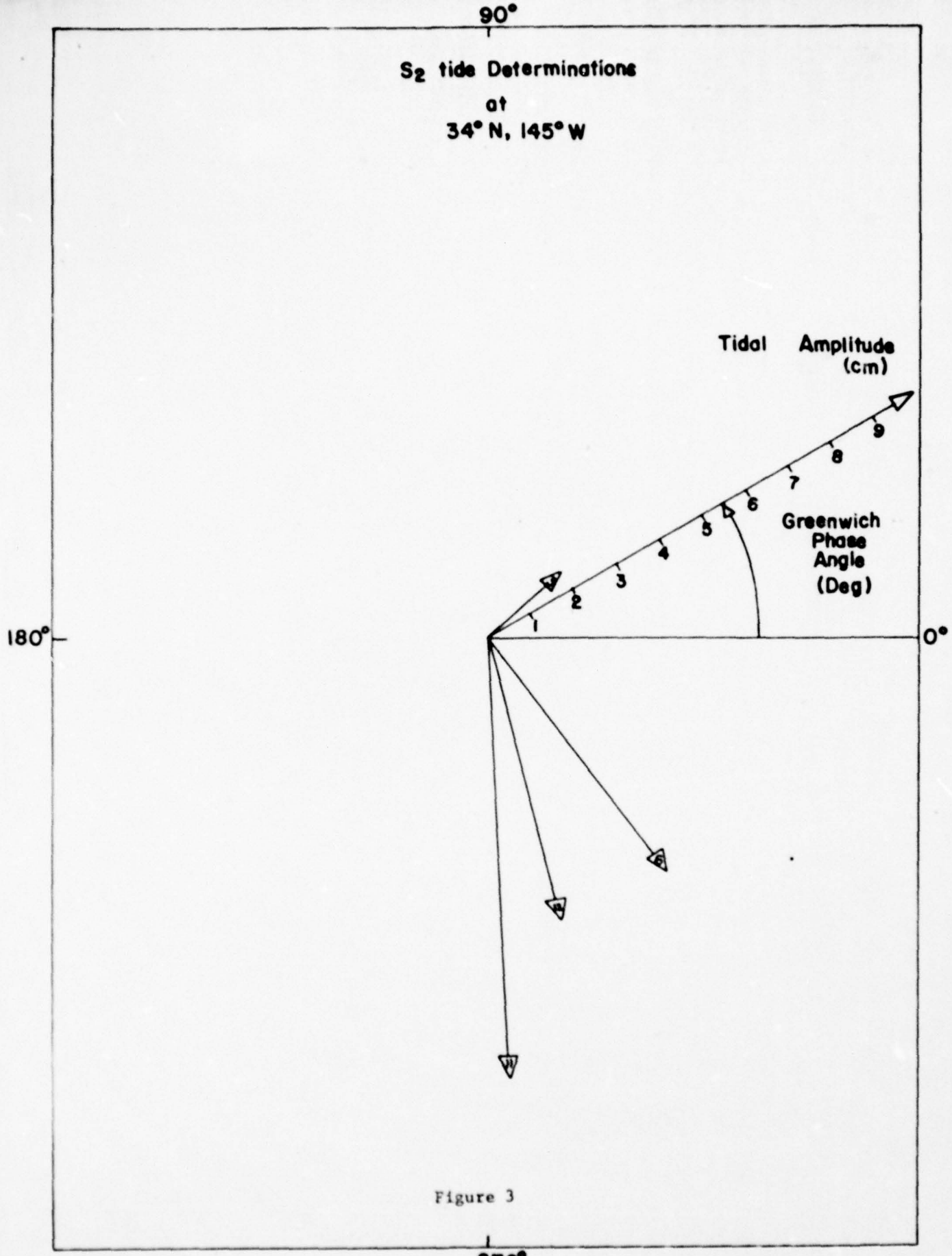
90°
S_2 tide Determinations
at
34° N, 145° W
Tidal Amplitude (cm)
1
2
3
4
5
6
7
8
9
Greenwich Phase Angle (Deg)
180°
0°
270°

Figure 3

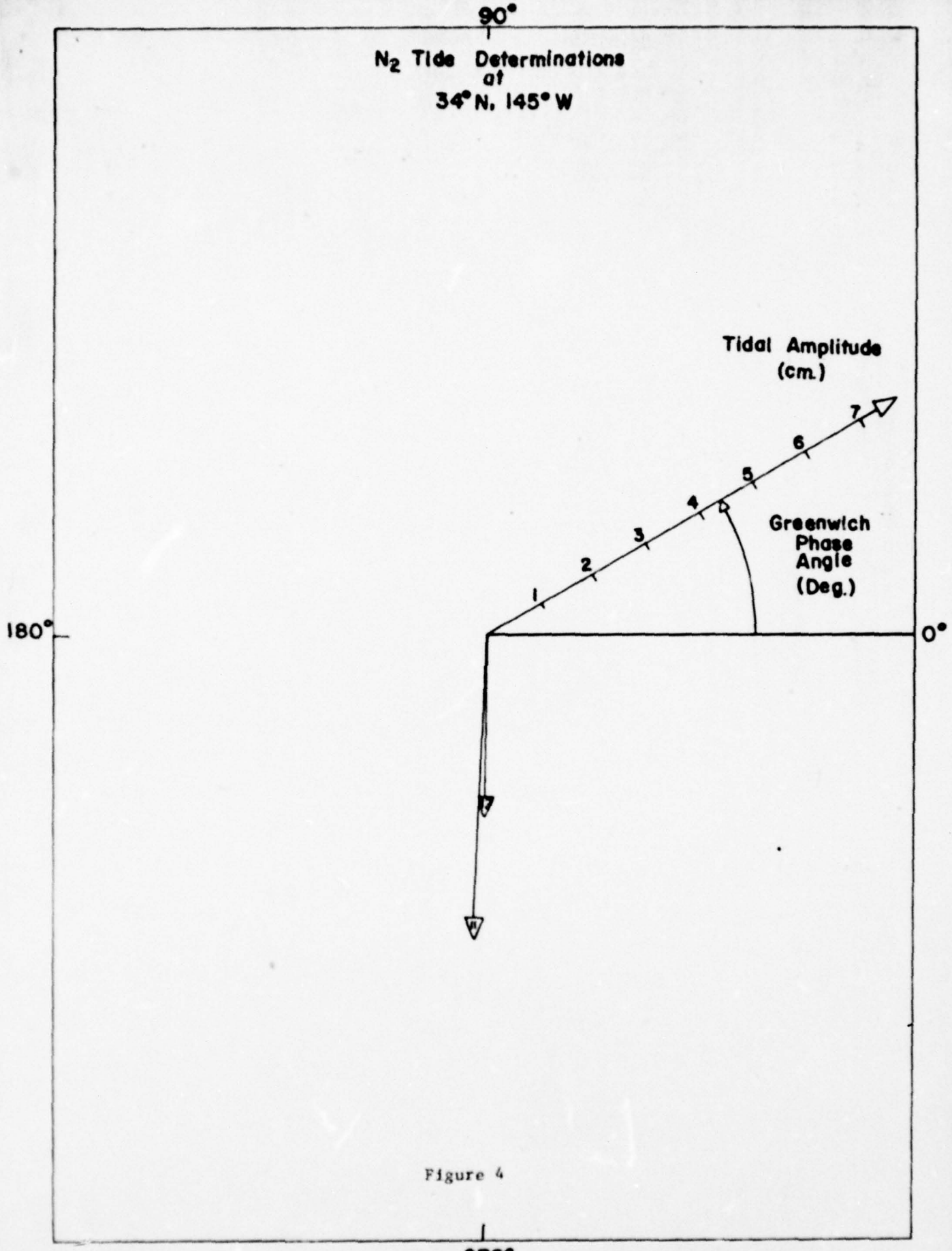
90°
N_2 Tide Determinations
at
34° N, 145° W
Tidal Amplitude
(cm.)
1
2
3
4
5
6
7
Greenwich
Phase
Angle
(Deg.)
180°
0°
270°

Figure 4

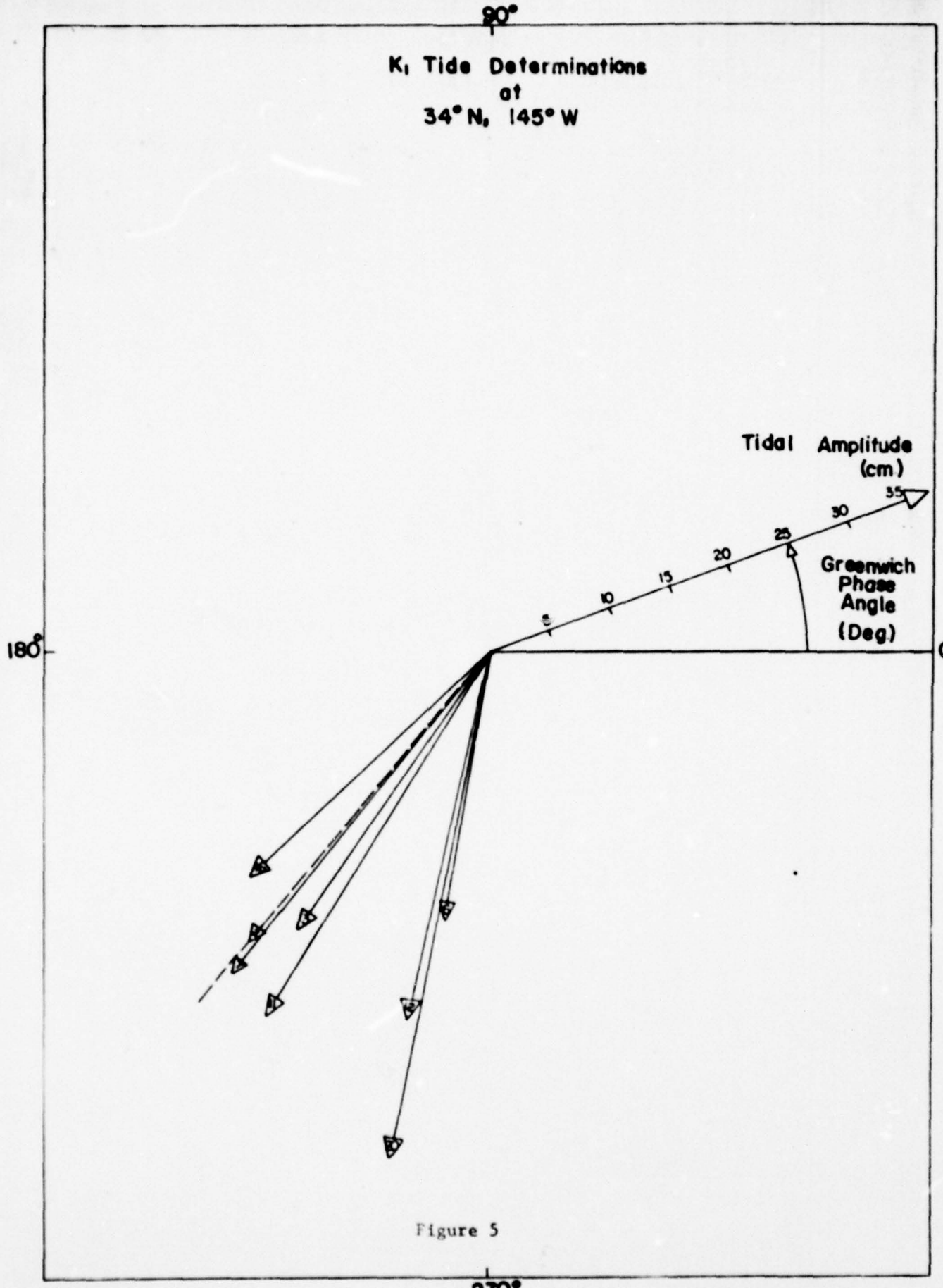
90°
K1 Tide Determinations
at
34° N, 145° W
Tidal Amplitude
(cm)
5
10
15
20
25
30
35
Greenwich
Phase
Angle
(Deg)
180°
0°
270°

Figure 5

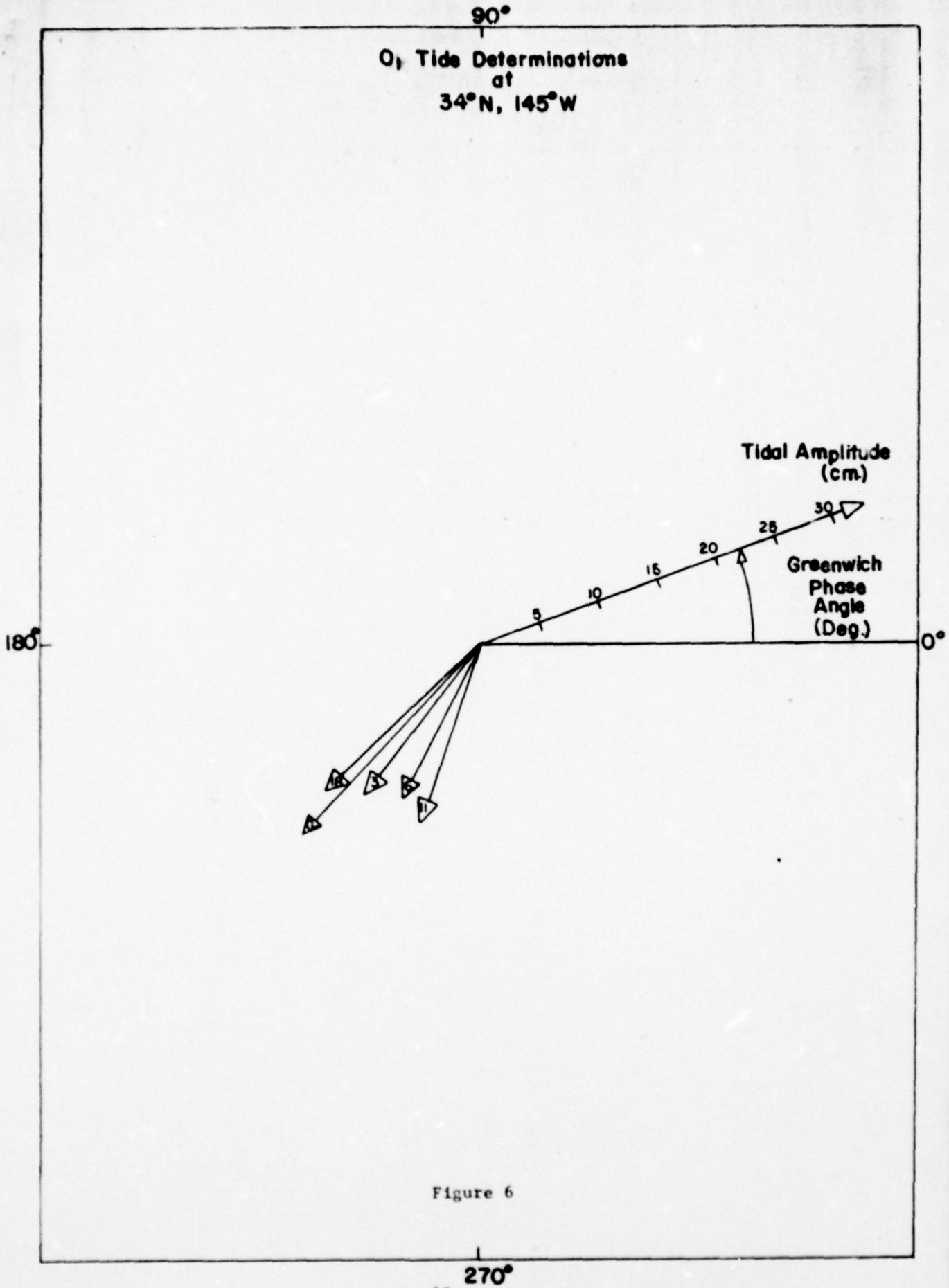
90°
O1 Tide Determinations
at
34°N, 145°W
Tidal Amplitude
(cm)
30
25
20
15
10
5
Greenwich
Phase
Angle
(Deg.)
180°
0°
270°

Figure 6

ALTIMETER DATA PROCESSING

The Northeast Pacific region is traversed by about 200 GEOS-3 altimeter data passes (see Figure 1), and about 400 Seasat altimeter data passes. Of these data, 184 GEOS-3 passes have already been processed, and the data, reduced to sea heights and corrected for orbit errors, is available from Goddard Space Flight Center.

To appreciate the key role of orbit error correction in the recovery of tidal information, it is helpful to review the altimeter measurement geometry shown in Figure 7. The altimeter measures the distance h between the instantaneous sea surface and the satellite along a line normal to the mean sea surface at a given time t. If the geocentric distance of the satellite, r_s, is known accurately at time t, then the geocentric distance to the instantaneous sea surface can be calculated. In particular, the sea surface height, S, above the reference ellipsoid can be calculated.

However, if there is some orbit error, i.e., r_s is not known accurately, then the corresponding sea surface height S will be in error and an erroneous ocean tide height will result. While it is theoretically possible (Zetler and Maul [1971]) to recover the tide parameters in the presence of orbit errors, Maul and Yanaway [1978] found that in practice, orbit errors were either too large or not random enough to permit successful tide parameter recovery. Other investigators [Won and Miller [1978] have also cited excessive orbit errors as a contributing factor in failure to achieve good tide parameter recovery from altimetry.

In this investigation, a unique process is used to remove orbit errors from the altimeter data. As it is not possible to know accurately the geocentric satellite distance r_s for each satellite pass, this quantity is replaced by a fictitious quantity which will result in the minimum deviation of the calculated sea surface height S from the modeled mean sea surface height N, over the length of the pass. The mean sea surface (or geoid) height, N, is calculated along the satellite subtrack, N(t), from a geopotential model such as GEM-7 (Wagner, et al [1976]). While N and S are not generally co-linear, to a good approximation they may be assumed so. The error in this

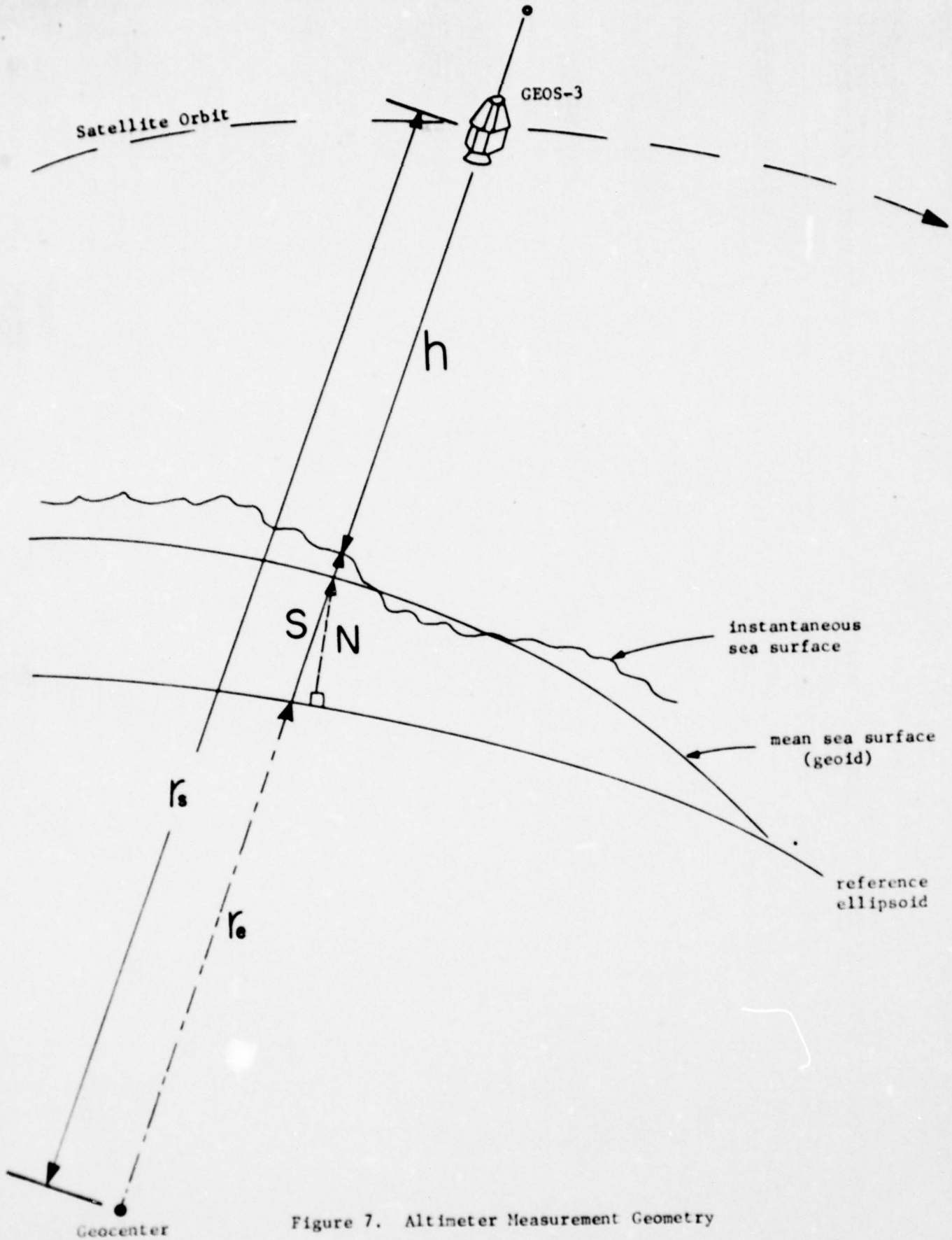

Figure 7. Altimeter Measurement Geometry

assumption is in the sub-centimeter range. The fictitious geocentric satellite distance r_s may be parameterized as a low order polynomial in t, e.g.,

$$r_s(t) \cong a + bt + ct^2$$

over the relatively short length of the satellite pass. This is a good approximation since only small fractions of a complete satellite orbit are to be fitted in each pass. The polynomial parameters, a, b, c, are then adjusted in a least squares process to minimize the difference between the calculated sea surface height, S(t)

$$S(t) = r_s(t) - h(t) - r_e(t)$$

and the calculated geoid height, N(t), along the length of the pass. Since each pass is thus fitted independently to the same model mean sea level surface, all orbit errors and any other phenomena which manifests itself like an orbit error (i.e., a bias or tilt) are removed and the sea height difference represents the true difference in sea surface height at the times of the intersecting passes. Each pass uses an independent set of fictitious polynomial parameters, and these have no real meaning or physical function whatever, except to accomplish the fitting of the sea surface heights to the model mean sea level. In this process, care must be taken in choosing the length of the pass which is fitted. In a very short pass, even the ocean tide signal appears as a bias and would be removed in this process. Therefore, all passes are chosen to be longer than 2500 km (6 minutes), which is sufficient to preserve the tidal information of the Northeast Pacific Ocean basin.

In actual practice, the adjustment and fitting of the sea surface height data is accomplished in a general purpose orbit determination program, using more sophisticated calculation of r_s, but the principal is the same. It is estimated that this process results in sea surface heights which are free of orbit error to within 20 centimeters (Brown et al [1977]).

CROSSOVER DATA PROCESSING

Once the altimeter data are converted to corrected sea surface heights, it is possible to parameterize differences in sea heights at crossovers in terms of phase differences of various components of the tides. The five largest tide components, M_2, K_1, S_2, O_1, and N_2, are estimated in a harmonic analysis of the crossover discrepancies. Referring to Figure 8, each sea height is expressed as the sum of contributions of all 5 components.

$$S(t) = \sum_{i=1}^{5} [a_i \sin w_i t + b_i \cos w_i t] = \sum_{i=1}^{5} A_i \cos(w_i t - \Phi_i) \qquad (1)$$

The sea height difference at the j^{th} crossover is thus parameterized by ten tide parameters, (two for each of the five components). It is given by

$$\Delta S_j = \sum_{i=1}^{5} [a_i(\sin w_i t_2 - \sin w_i t_1) + b_i(\cos w_i t_2 - \cos w_i t_1)] \qquad (2)$$

where w_i are the frequencies of the tidal components, and a_i and b_i are the tidal parameters. The amplitude A_i and phase Φ_i of a particular tide component are given by

$$A_i = \sqrt{a_i^2 + b_i^2}$$

and

$$\Phi_i = \tan^{-1}\left(\frac{a_i}{b_i}\right)$$

Clearly, to solve for the ten unknown parameters, we need at least 10 independent measurements of ΔS at a particular location. This is difficult to achieve, given that the GEOS-3 satellite orbit never exactly repeats. However, it does come close to repeating (within 1/2 degree) every fortnight. Thus, it is not

TIDAL MEASUREMENT GEOMETRY

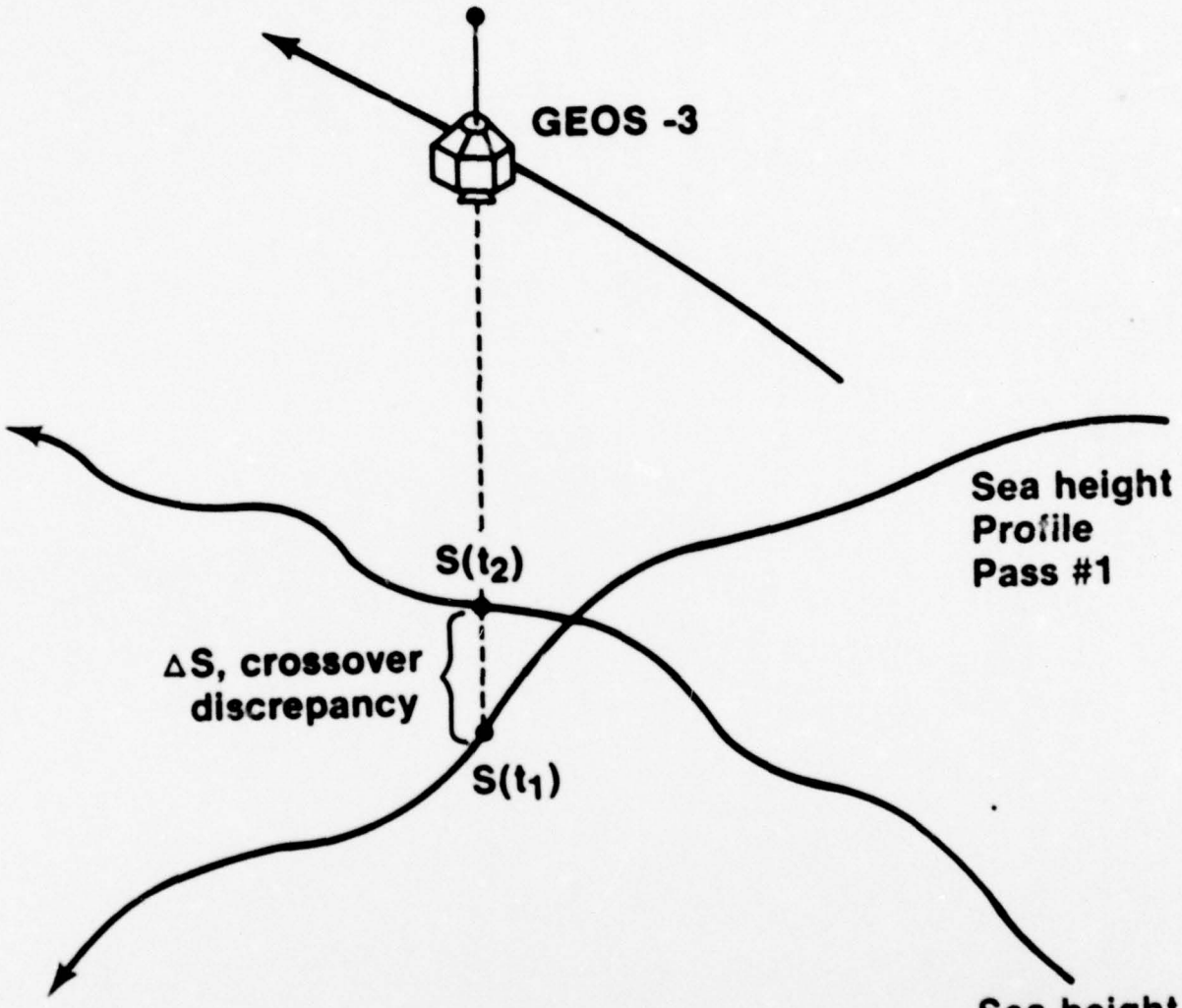

$$S(t_2) = \sum_i a_i \sin \omega_i t_2 + b_i \cos \omega_i t_2$$

$$S(t_1) = \sum_i a_i \sin \omega_i t_1 + b_i \cos \omega_i t_1$$

$$\Delta S = \sum_i a_i (\sin \omega_i t_2 - \sin \omega_i t_1) + b_i (\cos \omega_i t_2 - \cos \omega_i t_1)$$

Figure 8

difficult to collect a sufficient number of crossovers within a few degrees of the desired location (see Figure 9). But one must assume that the tide amplitude and phase are constant over the area spanned by this collection of crossovers.

Further assumptions are necessitated by the fact that one does not collect a sufficient number of crossovers instantaneously. Due to the power limitations of the GEOS-3 satellite, the altimeter did not operate continuously. Therefore, there may be a time lapse of a year or more between t_2 and t_1 at a given crossover (see Figure 9). Thus one must assume that there are no secular effects on the tides which are significant in the time span needed to collect sufficient crossovers.

Such long phase delays make accurate knowledge of the tidal component periods more important also. An error of about one part in 10^6 in the period of a semi-diurnal component is sufficient to cause a 2.5^o error in phase angle after a year. Tide component periods used in this investigation are accurate to better than 1 part in 10^8.

Other factors that change with time must also be carefully monitored. For example, while the altimeter is largely insensitive to sea state (wind waves, swells, etc.), a significant wave height (SWH) of 10 m or more can cause 0.5 m to 1 m error in altitude readings (Hofmeister, et al [1976]). It is therefore important that the sea state conditions be rather calm (SWH < 3m) for good tide determinations.

The GEOS-3 and SEASAT-1 altimeter data distributions have been examined to determine the number and location of potential tide solution locations in the Northeast Pacific. Locations at which concentrations of twenty or more crossovers exist within a small local area (less than about 5^o by 5^o area) from passes longer than 2500 km have been identified for both satellites. Twenty-six tide solution areas which have been identified from 98 GEOS-3 passes are shown by the circles in Figure 10. The solid triangles in Figure 10 represent the solution areas of highest crossover density from the SEASAT-1 altimeter data. Since the SEASAT satellite was placed in a 3-day repeating orbit near the end of its lifetime, crossover concentrations in excess of 100 per 6 min. by 6 min. area were generated at these locations. Many other solution locations which have fewer crossovers could be identified from the

TYPICAL MEASUREMENT DISTRIBUTION FOR A LOCAL TIDAL SOLUTION

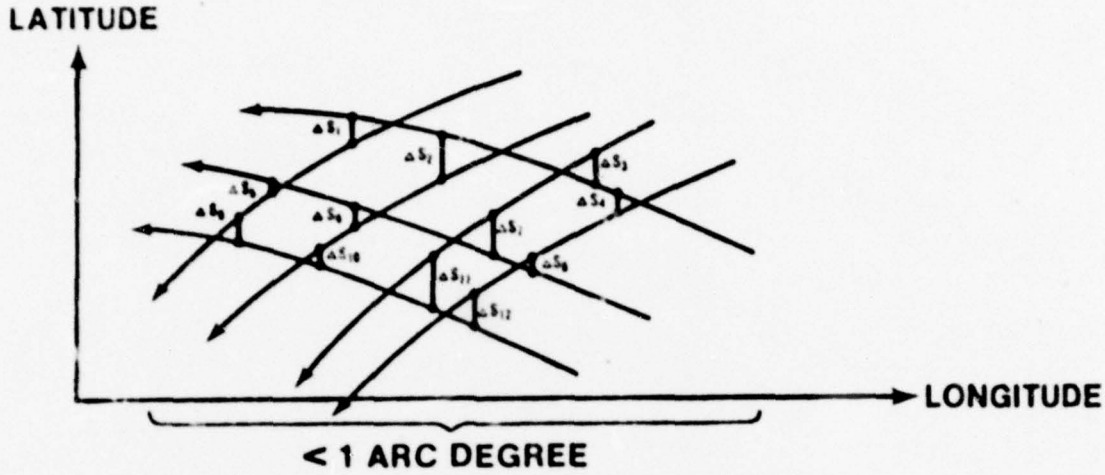

SAMPLING OF LOCAL TIDAL SIGNAL

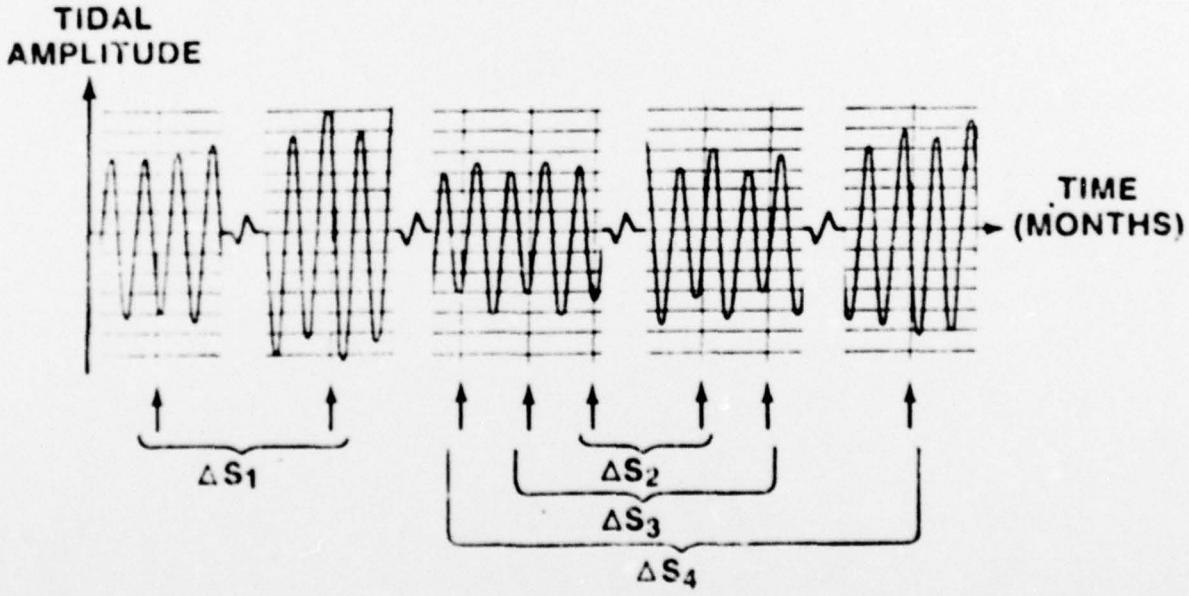

Figure 9

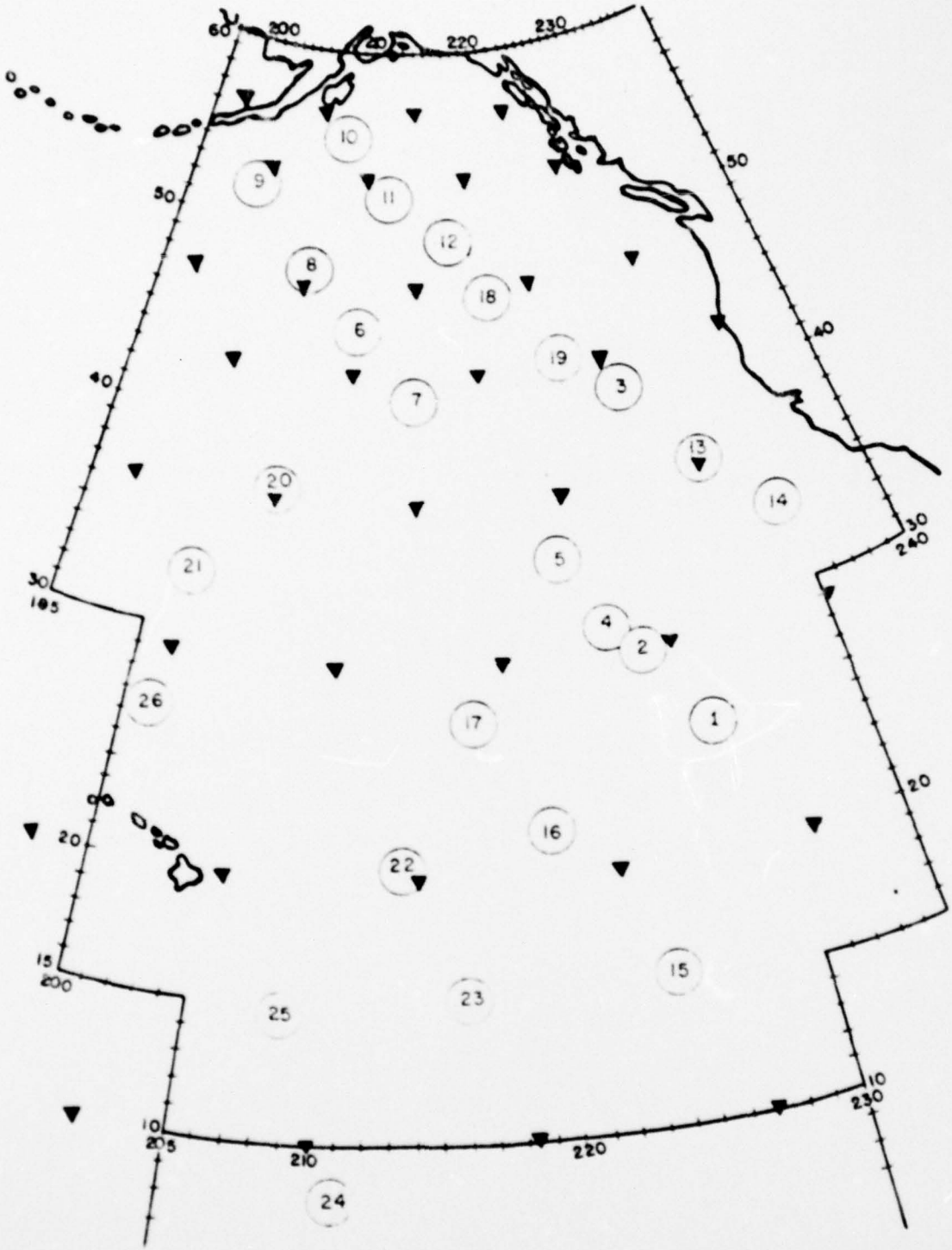

Figure 10. Locations for Tide Solutions

SEASAT-1 data distribution, but these 37 will provide potentially the highest quality solutions. The total of 63 tide solution locations identified in Figure 10 provide for a tide determination roughly every 5 degrees.

The determination of tide parameters, a_i and b_i, at a given location is a simple least squares adjustment to minimize the crossover discrepancies ΔS_j. Normal equations are formed for each of the solution locations. If we rewrite equation 2 in terms of matrices, we have

$$\vec{\Delta S} = [A]\,\vec{X}$$

where

$$A_{ij} \text{ is } \sin w_j t_i^2 - \sin w_j t_i^1, \text{ or, } \cos w_j t_j^2 - \cos w_j t_j^1$$

and

$$\vec{X} \text{ is } \begin{bmatrix} a_i \\ b_i \end{bmatrix}$$

The resulting normal equation

$$[A]^T\ \vec{\Delta S} = [A]^T\,[A]\,\vec{X}$$

has as its solution

$$\vec{X} = \left[[A]^T\,[A]\right]^{-1}[A]^T\,\vec{\Delta S}$$

PRELIMINARY TIDE SOLUTIONS

Tide determinations have been made to date at eight of the 26 GEOS-3 solution locations shown in Figure 10. These solutions are of a preliminary nature, but serve to point out some problem areas as well as some encouraging new approaches to be investigated in a subsequent study.

Table 1 shows the results of tide solutions at several of these locations for up to 5 tide components. All of the solutions are standard unconstrained, unweighted least squares solutions. The first two solutions, TMA and TMB, illustrate a phenomenon which may be called dilution of the strength of the solution. Both solutions result in a reduction in the RMS of crossover residuals, but at the expense of ridiculously large tide amplitudes. The determinant values are also relatively small (even negative in the case of TMB) which further indicates a weak or ill-conditioned solution. This situation comes about when the number of unknowns (10) approaches the number of observations (27 and 25). It is improved as the number of unknowns is decreased. For example, note the decrease in amplitude and increase in determinant value as the number of components solved for in location 2 is reduced (solutions TM2, TM5, TM52, and TMB2). The value for M_2 achieved in TMB2 is in fair agreement with bottom pressure gauge results reported by Munk et al [1970] for the nearby Filloux gauge (.19 m amplitude and 107.14° Greenwich phase angle).

This approach of reducing the unknowns is not generally recommended because the several frequencies represented in the 5 tide components are not distinctive enough that the parameters of each component are uncorrelated. Thus, if a given component, say N_2 is not solved for, its contribution to the crossover discrepancies is absorbed erroneously by another component whose parameters have a high cross-correlation with N_2. This is seen in the dramatic change of parameter values caused by deletion of the O_1 component in solutions TM2 and TM5. In solution TM2, the correlation between the O_1 parameters and other parameters ranges from .81 to .91.

The addition of further observations also strengthens the solution, as shown in solution ADD, but not as dramatically as reducing the unknowns. The normal equations of solutions TMA and TMB were added and solved to produce ADD. This is equivalent to a single solution of 52 cross-over discrepancies. Note

TABLE 1

PRELIMINARY TIDE SOLUTIONS

Solution	Location	Passes	Cross-overs	Determinant	Amplitude (m.) [Greewich Phase Angle (deg.)] M_2	K_1	S_2	O_1	N_2	Residual RMS (m) Before/After
TMA	1	11	27	7×10^{9}	7.0[8°]	5.0[333°]	5.6(231°)	7.4(295°)	14.7(299°)	3.85/1.15
TMB	2	10	25	-4.3×10^{5}	37.6(240°)	30.2(277°)	32.2(212°)	60.3(130°)	20.5(156°)	2.99/0.61
TM2	2	10	25	1.8×10^{20}	2.5(217°)	2.9(255°)	3.0(354°)	8.1(146°)		/0.50
TM5	2	10	25	4.2×10^{31}	1.0(53°)	1.7(35°)	1.2(116°)			/1.50
TM52	2	10	25		1.0(43°)	2.5(33°)				
TMB2	2	10	25		.5(67°)					
ADD	1&2	21	52	5.8×10^{14}	1.3(177°)	1.1(327°)	1.8(89°)	3.3(212°)	.6(68°)	
TM3	3	16	60	4.9×10^{15}	2.1(18°)	1.1(297°)	1.1(230°)	1.1(247°)	.6(310°)	3.77/2.98
TM3L	3	13	30	2.5×10^{13}	.3(184°)	1.1(0°)	1.0(102°)	1.0(125°)	.6(120°)	3.01/1.88
TO4	4	10	24		.7(278°)					
TO4B	4	10	24		.5(284°)					
TO8	8	13	34	1.1×10^{12}	.4(252°)	1.3(350°)	.2(252°)	1.2(136°)	.2(191°)	1.52/1.05

that the determinant value increased and the tide component amplitudes decreased to more reasonable levels. This is a preferred technique for improving the quality of the tide solutions. In this case, the addition of observations is misleading, since they are not from the same immediate area. In ADD, the crossover locations range from 22.5° to 30.5°N and 224°E to 229°E. When SEASAT data are processed, the crossovers available for a given location are expected to increase by an order of magnitude, with a corresponding increase in quality of the solution.

Another preferred technique for improving solutions is to improve the quality of the observations. In a few solutions, it was noticed that the crossover discrepancy values for a given pass were systematically different from those of other passes, e.g., all crossovers associated with a given pass might have a significant non-zero mean. This could happen if orbit error removal was incomplete for some reason. When these crossovers are removed from the solution, the solution values became more reasonable, despite the reduced number of observations. For example, solution TM3 for location 3 had 60 crossovers, but those of 3 passes appeared to be systematically offset from the others. When these crossovers were removed, as in solution TM3L, the amplitude of the M_2 term dropped from 2.1 to .3 meters. The RMS of crossover discrepancies also improved more in TM3L than in TM3, despite the loss of 30 observations. Apparently, biases in the crossover discrepancies alias significantly with tide parameters.

Ideally, one would like to be able to correct the biases in faulty passes while still retaining the tidal information. This may be effected by adding pass bias terms to the observation equation. In this case, equation (2) becomes

$$S_j = O_2 - O_1 + \sum_{i=1}^{5} \left[a_i(\sin w_i t_2 - \sin w_i t_1) + b_i(\cos w_i t_2 - \cos w_i t_i) \right] \quad (3)$$

Normal matrices formed from these equations would have, in addition to the 10 tide parameters, one pass bias for each pass (one pass bias must be held fixed to avoid a singular matrix). This has the effect of diluting the strength of the solution if all parameters are solved simultaneously, but

it is feasible to solve for the biases independently and correct the crossover discrepancies before executing the tidal solution. This was attempted in solution T04B. Comparing with solution T04, before pass bias correction, we see that the most significant effect is the reduction of the amplitude of the M_2 component. Not much phase angle change occurs at all.

Finally, the solution for location 8 is presented to indicate that there are data which yield well-behaved solutions without any remedial treatment. This is a case where the input data are not biased (initial RMS of crossover is small, $\pm$ 1.52 m), and there are sufficient crossovers (34) to give a strong solution (determinant is rather large at 1.1×10^{12}).

It is too soon to begin comparison of the recovered tide parameter values with those of other investigators, but the preliminary results are encouraging.

CONCLUSIONS AND RECOMMENDATIONS

Knowledge of tides in the Northeast Pacific Ocean is fairly uncertain at present, but the advent of satellite altimetry data from the GEOS-3 and SEASAT satellites promise the possibility of direct measurements of tides in this area. From these data one can determine tide constants on a 5^{o} by 5^{o} grid over all the deep ocean. Analysis of preliminary altimeter tide solutions have underscored the necessity for complete removal of all orbit type bias errors from the data before attempting to solve for tides. Fortunately, techniques have been developed for editing or correcting biased data and obtaining good quality tidal solutions. The future processing of SEASAT data will yield much higher quality solutions owing to the high density of crossovers which accrues from the SEASAT repeating orbit, and the more accurate SEASAT altimeter data.

In the near future, the remaining GEOS-3 crossover data will be processed and corrected for biases and solutions will be achieved for all 26 solution areas. Processing of SEASAT altimeter data is expected to begin in November of 1979. Comparison and validation of various tide determinations will follow the construction of tide solutions from the SEASAT data.

REFERENCES CITED

Bogdanov, K.T., 1961a, New charts of co-tidal lines of semi-diurnal tidal waves (M_2 and S_2) for the Pacific Ocean, Doklady Akademii nauk SSSR, v. 138, no. 2, pp. 441-444.

Bogdanov, K.T., 1961b, New charts of co-tidal lines of the diurnal tide (K_1 and O_1) for the Pacific Ocean, Doklady Akademii nauk SSSR, v. 139, no. 3, pp. 713-716.

Bogdanov, K.T., Kim, K.V., and Magarik, V.A., 1964, Numerical solution of tide hydrodynamic equations by means of BESM-2 electronic computer for the Pacific area, Akademia nauk SSSR, Trudy Institute Okean ologii, 75, pp. 73-98.

Brown, R.D., and Lo, H.H., 1979, Definition of tides in shelf waters from altimetry, (abstract) EOS, Transactions of the American Geophysical Union.

Brown, R.D., Masters, T.G., and Kahn, W.D., 1973, GEOS-3 altimeter data analysis (abstract) EOS, Transactions of the American Geophysical Union, v. 57, no. 12, p. 900.

Dietrich, G., 1944, Die schwingung ssysteme der halb-und eintagigen tiden in den ozeanen, Veroffentl. Inst. Meereskunde Univ. Berlin, A41, pp. 7-68.

Estes, R.H., 1979, A computer software system for the generation of global ocean tides including self-gravitation and crustal loading effects, NASA Goddard Space Flight Center, Preprint X-920-77-82.

Gallagher, B.S., K.M. Shimadu, F.I. Gonzalez, and E.D. Stroup, 1971, Tides and Currents in Fanning Atoll Lagoon, Pacific Science, 25, pp. 191-205.

Gordeev, R.G., Kagan, B.A., and Polyakov, E.V., 1977, The effects of loading and self-attraction on global ocean tides: the model and the results of a numerical experiment, J. of Physical Oceanography, v. 7, no. 2, pp. 161-170.

Harris, R.A., 1904, Manual of tides, Parts 1 to 5, Appendices to U.S. Coast and Geodetic Survey Reports, Washington, D.C.

Hendershott, M.C., 1973, Ocean tides, EOS, Transactions of the American Geophysical Union, v. 54, no. 2.

Hendershott, M.C., 1972, The effects of solid earth deformation on global ocean tides, Geophysical Journal Roy. Astron. Soc., v. 29, pp. 389-403.

Hendershott, M.C., 1966, The numerical integration of Laplace's tidal equations in idealized ocean basins, Prac. Symp. on Math-hydrodynamical Investigations of Physical Processes in the Sea, Moscow.

Irish, J., Munk, W., and Snodgrass, F., 1971, M_2 amphidrome in the Northeast Pacific, Geophysical Fluid Dynamics, v. 2, pp. 355-360.

Kuo, J.T., and Jachens, R.C., 1977a, Indirect mapping ocean tides by solving the inverse problem for the tidal gravity observations, Ann. Geophys., t. 33, fasc. 1/2, pp. 73-82.

Kuo, J.T., Jachens, R.C., and Lee, S.S., 1979b, The Northeastern Pacific O_1 and the North Atlantic M_2 ocean tides as derived from inversion, presented at the Eighth International Symposium on Earth Tides, Bonn, F.R.G., September 19-24, 1979.

Luther, D.S., and Wunsch, C., 1975, Tidal charts of the Central Pacific Ocean, J. of Physical Oceanography, v. 5, pp. 222-230.

Maul, G.A., and Yanaway, A., 1978, Deep sea tides determination from GEOS-3, NASA Wallops Flight Center Contractor Report 141435.

Munk, W.H., Snodgrass, F., and Wimbush, M., 1970, Tide off-shore: Transition from California coastal to deep sea waters, Geophysical Fluid Dyn. 1, pp. 161-235.

Pekeris, C.L., and Accad, Y., 1969, Solution of LaPlace's equations for the M_2 tide in the world oceans, Phil. Trans. Roy. Soc. London, A. 265, pp. 413-436.

Rapatz, W.S., and Huggett, W.S., 1977, Pacific Ocean offshore tidal program, Proceedings of the Fifteenth International Congress of Surveyors, Commission 4, Hydrographic Surveying, pp. 179-195, June 9-14, 1977.

Tiron, K.D., Sergeev, Y.N., and Michurin, A.N., 1967, Tidal charts of the Pacific, Atlantic, and Indian Oceans, Vestnik of Leningrad University, v. 24, pp. 122-135.

Wagner, C.A., Lerch, F.J., Brownd, J.E., and Richardson, J.A., 1976, Improvement in geopotential derived from satellite and surface data (GEM 7 and 8), NASA Goddard Space Flight Center X-921-76-20.

Won, I.J., and Miller, L.S., 1978, Oceanic geoid and tides obtained from GEOS-3 satellite data in the Northwestern Atlantic Ocean, NASA Wallops Station Contractor Report 156845.

Won, I.J., Kuo, J.T., and Jachens, R.C., 1978, Mapping ocean tides with satellites: A computer simulation, Journal of Geophys. Res., v. 83, no. B12, pp. 5947-5960.

Zahel, W., 1970, Die reproduktion gezeitenbedingter bewegungsvorgange im weltozean mittels des hydrodynamisch-numerischen verfahrens, Mitt Inst. Meereskunke der Univ. Hamburg, v. 17.

Zetler, B.D., and Maul, G.A., 1971, Precision requirements for a spacecraft tide programs, Journal of Geophys. Res., 76(27), pp. 6601-6605.

Zetler, B.D, Munk, W., Mofjeld, Brown, W., and Dormer, F., 1975, MODE tides, Journal of Physical Oceanography, v. 5, pp. 430-441.

SECURITY CLASSIFICATION OF THIS PAGE (When Data Entered)

REPORT DOCUMENTATION PAGE

READ INSTRUCTIONS BEFORE COMPLETING FORM

1. REPORT NUMBER	2. GOVT ACCESSION NO. / 3. RECIPIENT'S CATALOG NUMBER
4. TITLE (and Subtitle): VALIDATION OF OCEAN TIDE MODELS FROM SATELLITE ALTIMETRY; Progress Report	5. TYPE OF REPORT & PERIOD COVERED: Interim, May 1978 to October 1978
	6. PERFORMING ORG. REPORT NUMBER
7. AUTHOR(s): R.D. Brown	8. CONTRACT OR GRANT NUMBER(s): N00014-79-C-0409
9. PERFORMING ORGANIZATION NAME AND ADDRESS: Phoenix Corporation, 1700 Old Meadow Road, McLean, Virginia 22102	10. PROGRAM ELEMENT, PROJECT, TASK AREA & WORK UNIT NUMBERS
11. CONTROLLING OFFICE NAME AND ADDRESS: Office of Naval Research, Earth Physics Program, 800 N. Quincy Street, Arlington, VA 22217	12. REPORT DATE: October 15, 1979 13. NUMBER OF PAGES: 33
14. MONITORING AGENCY NAME & ADDRESS(if different from Controlling Office)	15. SECURITY CLASS. (of this report): Unclassified 15a. DECLASSIFICATION/DOWNGRADING SCHEDULE

16. DISTRIBUTION STATEMENT (of this Report)

17. DISTRIBUTION STATEMENT (of the abstract entered in Block 20, if different from Report)

18. SUPPLEMENTARY NOTES

To be presented at the Annual Fall Meeting of the American Geophysical Union, San Francisco, December 3-7, 1979

19. KEY WORDS (Continue on reverse side if necessary and identify by block number)

Ocean Tides
Satellite Altimetry
SEASAT

20. ABSTRACT (Continue on reverse side if necessary and identify by block number)

Tides in the deep ocean can be determined directly from satellite altimetry, completely independent of assumptions about earth tides, bottom topography and coastal geometry and thus free of the uncertainties which plague numerical tide models. Existing tide models differ by 1 meter or more in the value of sea surface height in the deep ocean at a given place and time. This uncertainty is a formidable obstacle to determination of a precise marine geoids from satellite altimetry. By harmonic analysis

DD FORM 1 JAN 73 1473 EDITION OF 1 NOV 65 IS OBSOLETE

SECURITY CLASSIFICATION OF THIS PAGE (When Data Entered)

cont

of the temporal changes in altimeter measurements at satellite subtrack crossover points, it is possible to solve for the amplitude and phase of harmonic tidal components. However, care must be exercised in the removal of satellite orbit errors, and in the selection of crossovers for sufficient observability of the phase angle of the harmonic tidal component. Preliminary tidal solutions in the Gulf of Alaska using the relatively sparse GEOS-3 altimeter data distribution show generally good agreement (20 cm in amplitude and 25 degrees in phase) with deep ocean bottom pressure gauge measurements and establish the feasibility of this technique. SEASAT altimeter data yields a much greater density of crossovers (400 plus per 1/2° by 1/2° area), making possible much better separation of individual harmonic components within the semi-diurnal and diurnal families. Five degree resolution on tidal charts of co-range and co-phase lines in the Gulf of Alaska are possible with the SEASAT data distribution.

deg